

Semi-coherent time of arrival estimation using regression

Alexander Apartsin^{a)}

Blavatnik School of Computer Science, Tel-Aviv University, Ramat-Aviv 69978, Israel

Leon N. Cooper

Physics Department, Brown University, Providence, Rhode Island 02912

Nathan Intrator^{b)}

Blavatnik School of Computer Science, Tel-Aviv University, Ramat-Aviv 69978, Israel

(Received 6 October 2011; revised 18 May 2012; accepted 29 May 2012)

Time of arrival (ToA) estimation is essential for many types of remote sensing applications including radar, sonar, and underground exploration. The standard method for ToA estimation employs a matched filter for computing the maximum likelihood estimator (MLE) for ToA. The accuracy of the MLE decreases rapidly whenever the amount of noise in a received signal rises above a certain threshold. This well-known threshold effect is unavoidable in several important applications due to various limitations on the power and the spectrum of a narrowband source pulse. A measurement performed in the presence of the threshold effect employs a receiver which operates in the semi-coherent state. Therefore, the conventional methods assuming a coherent state receiver should be adapted to the semi-coherent case. In this paper, a biosonar-inspired method for the semi-coherent ToA estimation is described. The method abandons the exploration of an echo signal by a single matched filter in favor of the analysis by multiple phase-shifted unmatched filters. Each phase-shifted unmatched filter gives rise to a biased ToA estimator. The described method uses regression for combining these estimators into a single unbiased ToA estimator that outperform the MLE in the presence of the threshold effect. © 2012 Acoustical Society of America. [http://dx.doi.org/10.1121/1.4730885]

PACS number(s): 43.60.Bf, 43.60.Np, 43.80.Ka, 43.60.Cg [JAS]

Pages: 832–837

I. INTRODUCTION

In remote sensing applications such as radar or sonar, the common scenario starts by a transmitter sending out a pulse waveform (ping) $s(t)$. The pulse is reflected from a target and a receiver picks it up at time t_0 . The estimated two-way travel time (lag) can be used to calculate the distance to the target assuming the speed of the pulse propagation in the medium is known.¹ The signal recorded at the receiver might be represented as

$$x(t) = d \cdot s(t - t_0) + n(t),$$

where $n(t)$ is additive white Gaussian noise that corrupts the signal. The $d \leq 1$ factor is used to account for all non-free space propagation losses (e.g., attenuation of the signal in the medium). The goal of the time of arrival (ToA) estimation is to produce an unbiased estimate $\hat{t}_0(x, s)$ that minimizes the mean square error (MSE):

$$\text{MSE} = E_{t_0, n} \left(t_0 - \hat{t}_0(x, s) \right)^2.$$

The standard method for ToA estimation is based on a matched filter.² The matched filter is applied by convolving

a received signal with the source waveform and in order to maximize the ratio of the peak signal power to the average noise power at the output. The output of the matched filter can be represented as

$$C(t) = x(t) \circ s(t) = s(t) \circ s(t) + n(t) \circ s(t) = R(t) + \eta(t),$$

where $R(t)$ is the source signal's autocorrelation function. Using the matched filter, the maximum likelihood estimator (MLE) for ToA could be constructed by selecting the position of the peak (global maximum) in the matched filter output:

$$\hat{t}_0(x, s) = \arg \max_t C(t).$$

The resulting estimator is unbiased and therefore its MSE can be bounded by the Cramer–Rao lower bound (CRLB):³

$$\text{MSE}(\hat{t}_0) = \text{Var}(\hat{t}_0) \geq \frac{1}{I(t)},$$

where $I(t)$ is a Fischer information matrix defined by

$$I(t) = -E \left[\frac{\partial^2 l(x, t)}{\partial t^2} \right]$$

and $l(x, t)$ is a log-likelihood function. The MLE is asymptotically efficient under some regularity conditions,⁴ meaning that it reaches CRLB when computed over a large sample which, in this case, is equivalent to a long (infinite)

^{a)}Author to whom correspondence should be addressed. Electronic mail: apartsin@tau.ac.il

^{b)}Also at Institute for Brain and Neural Systems, Brown University, Providence, RI 02912.

observation duration of the received signals. It turns out that the finite set behavior of most non-linear estimators is not quite understood and their performance usually analyzed by designing appropriate and hopefully tighter low bounds such as Ziv–Zakai bounds and a family of Barankin bounds.^{5,6} The Barankin bound,^{7,8} for instance, helps to account for the threshold effect which causes a rapid increase in the mean squared error (MSE) of the finite sample ML ToA estimator whenever the signal-to-noise ratio (SNR) falls below a certain threshold.⁹

For narrowband signals, the threshold effect is triggered whenever additive noise makes a side lobe of the signal autocorrelation function to appear as the global maximum in the MF output.^{10,20} In the absence of noise, the maximum value of $C(t)$ is achieved at $t = t_0$. As the level of noise increases, the filtered noise $\eta(t)$ may cause a slight shift in the location of the peak of $C(t)$. However, at high noise levels, a location around one of the side lobes of $R(t)$ may occasionally become the global maximum of $C(t)$. A side lobe of the autocorrelation function mistakenly taken as its global maximum is the major reason behind deterioration in the accuracy of MLE ToA estimator in the presence of the threshold effect.¹¹

Several characteristics of a source signal waveform affect the severity of the threshold effect. The relative height of the side lobes of the autocorrelation function compared to the height of its main lobe and the distance between side lobes and the main lobe have the crucial impact. In particular, since the height of the side lobes of the autocorrelation function is affected by the pulse bandwidth, the threshold effect is stronger for low bandwidth pulses.

There are a few methods for improving near-the-threshold (semi-coherent) ToA estimation. Beyond apodization and increasing the power of a pulse for improving SNR at a receiver,¹² one can average over several measurements corrupted by high, but independent, additive noise. Then the individual estimates could be combined (fused) together to create a noise resilient estimator. In the presence of the threshold effect, the fusion methods also require special treatment. For instance, it has been shown that for a semi-coherent estimation, some robust fusion statistics (median, mode) give better results compared to the simple averaging (mean).¹³

Interestingly, some echolocating animals are remarkably good in processing reflected acoustic signals near or at the threshold SNR zone. Echolocation, also called biosonar, is biological sonar used by several mammals such as bats, dolphins, and whales. Echolocating animals emit pings out to the environment, and listen to the echoes of those pings that are reflected from objects in the environment. Animals use these echoes to locate, range, and identify objects. It appears that some echolocating animals could use their biosonar capabilities with striking precision and can operate at very low SNR levels. For instance, FM bats are capable of perceiving objects with a resolution of the order of millimeters and fractions of millimeters.¹⁴ In much more harsh underground environment a blind mole rat uses sonar-like exploration of its surroundings.¹⁵ This rat, which lives underground and has no functioning eyes, generates ground stimulation

by banging its head on the wall of its tunnels. A mole rat can dig a tunnel 300ft long in one night while detecting and avoiding voids and obstacles (e.g., stones) that are several feet ahead.¹⁵

The ability of echolocating animals to extract useful information from very weak echo returns apparently relies on massive parallel processing of a returned signal by a large amount of individual biological processing units.¹⁶ A bank of filters with specific impulse responses is frequently used for modeling of individual processing components. The outputs of multiple filters are fused together by different schemes to obtain a combined estimation. Following this approach, our method employs a filter bank of phase-shifted unmatched filters for parallel analysis of a returned signal. In Refs. 10 and 11 we have used a pair of such filters for deriving a SNR-dependant semi-coherent ToA estimator which requires knowledge of operational SNR level which should be estimated separately.¹⁷

In this work, we continue with the biosonar approach to design a robust estimation method especially suited for ToA estimation in the presence of the threshold effect. Using a family of phase-shifted unmatched filters, we construct a feature space for characterizing an echo return signal. Then, using a vector of values obtained by these unmatched filters, we train a regression model to predict an error (bias) introduced to the MLE by an outlier event. Using the predicted value of the bias, the MLE is corrected by this value resulting in the estimator that has smaller MSE for a range of near-the-threshold SNR values. Since the regression model is trained using a mix of samples generated using different SNR values, no prior knowledge on operational SNR is required for the estimation. Using the proposed method, the effective range, and power efficiency of a remote sensing application could be significantly improved.

The rest of the paper is organized as follows. The next section presents phase-shifted unmatched filters and biased estimators which are obtained using these filters. Some interesting properties of these filters and estimators are discussed, extending previous presentation on the subject.¹¹ In Sec. III, the regression-based fusion method is described for extracting unbiased ToA estimated from a feature vector generated by phase-shifted unmatched filters. The concluding section discusses simulation results and some possible extensions of the proposed method.

II. PHASE-SHIFTED UNMATCHED FILTERS AND BIASED ESTIMATORS

A phase-shifted unmatched filter pair is generated by shifting a phase of every harmonic in the source signal using a phase shift value of the same magnitude but of opposite sign $\pm\varphi$. The phase-shifting operation can be performed using the Hilbert transform

$$S_{\pm\varphi}(t) = \cos(\pm\varphi)s(t) - \sin(\pm\varphi)\hat{s}(t),$$

where $s(t)$ is a source waveform and $\hat{s}(t)$ is its Hilbert transform. Then the result of convolution of the received signal

with the pair of phase-shifted unmatched filters has the following form:

$$\begin{aligned} C_{\pm\varphi}(t) &= x(t) \circ s_{\pm\varphi}(t) = s(t) \circ s_{\pm\varphi}(t) + \eta(t) \circ s_{\pm\varphi}(t) \\ &= R_{\pm\varphi}(t) + N_{\pm\varphi}(t), \end{aligned}$$

where $R_{\pm\varphi}(t)$ are cross-correlations between the source waveform and its phase-shifted replicas and $N_{\pm\varphi}(t)$ is a filtered noise. The cross-correlation of unmatched filter with the source signal has side lobes of different height.¹¹ This property allows one to construct a pair of ToA estimators that are only partially correlated. In particular, the pair of ToA estimators corresponding to a pair of phase-shifted unmatched filters could be defined by taking the position of the peak in the filter output

$$\hat{t}_{\pm\varphi}(x, s) = \arg \max_t C_{\pm\varphi}(t).$$

As will be shown below, each estimator in the resulting pair has a bias toward the higher side lobe of cross-correlation function. The magnitude of the bias is equal for both estimators but has opposite sign. The magnitude of the bias is greater for lower SNR values, as the probability of an outlier (a side lobe mistakenly taken for the main peak) is greater. A biased estimator constructed using phase-shifted unmatched filters is inferior to the optimal matched filter³ MLE mostly due to the appearance of a strong bias component in MSE. However, these biased estimators are not completely correlated for a range of SNR values near the threshold. Therefore, a pair of biased estimators with symmetrical bias can be averaged to produce an unbiased estimator:

$$\hat{t}_{\varphi}(x, s) = \frac{1}{2} (\hat{t}_{\pm\varphi}(x, s) + \hat{t}_{-\varphi}(x, s)).$$

For a fixed value of the phase shift, the estimator above will produce lower MSE than an MF-based estimator for a range of SNR values provided the gain obtained by averaging partially correlated estimators would outplay the loss due to the slight widening of the main peak of the cross-correlation functions. Assuming that the range of operational SNR values is known, the best phase shift value could be selected using simulations during the calibration phase to match a particular environment. In Ref. 2 a large number of simulations using different values of SNR and phase shift values were performed and the phase shift value corresponding to the minimal MSE was selected for each SNR value.

To obtain some insight regarding the behavior of biased estimators, we analyze the effect of the phase shift value on the estimator's bias and the correlation among the estimator pair. We carry out the analysis using a simple three-point model that considers filtered noise and cross-correlation function values only near the peak and two closest side lobes of the cross-correlation function.

First, we estimate the bias of an estimator constructed using a phase-shifted unmatched filter. Let us denote by $p_{+1}^{\pm\varphi}$ and $p_{-1}^{\pm\varphi}$ the probabilities that the maximum will fall on the left or on the right side lobe, respectively. The distance between neighboring peaks of the cross-correlation function

is equal to $2\pi/w$, where ω is the angular central frequency of a narrowband source signal. Then the bias for the estimator could be expressed as

$$\begin{aligned} b_{\pm\varphi} &= E\hat{t}_{\pm\varphi}(x, s) \\ &= p_{-1}^{\pm\varphi} \cdot (\pm\varphi/\omega - 2\pi/\omega) + p_{+1}^{\pm\varphi} \cdot (\pm\varphi/\omega + 2\pi/\omega) \\ &\quad + (1 - p_{-1}^{\pm\varphi} - p_{+1}^{\pm\varphi}) \cdot (\pm\varphi/\omega), \\ b_{\pm\varphi} &= \frac{2\pi}{\omega} (p_{+1}^{\pm\varphi} - p_{-1}^{\pm\varphi}) \pm \varphi/\omega = \frac{2\pi\Delta p_{\varphi}}{\omega} \pm \varphi/\omega. \end{aligned}$$

Figure 1 shows p_0^{φ} and Δp^{φ} for a range of phases and SNR levels. Using these values and the expression above, the bias of estimators for different values of a phase shift and for different SNR values is shown at Fig. 2 (left). Comparing this computed bias with the actual bias lines obtained by simulation as shown in Fig. 2 (right), it can be seen that the three-point model allows for a good prediction of a bias value. Since $p_{+1}^{+\varphi} = p_{-1}^{-\varphi}$ and $p_{-1}^{-\varphi} = p_{+1}^{+\varphi}$, it follows that $b_{+\varphi} + b_{-\varphi} = 0$ and therefore the average of two biased estimators generated using opposite phase shift values is unbiased. Using the same notation, the MSE of a MFMLE is

$$e_0 = p_{-1}(-2\pi/\omega)^2 + p_{+1}(+2\pi/\omega)^2 = \frac{4\pi^2}{\omega^2} (1 - p_0).$$

For a phase-shifted version, the MSE is

$$\begin{aligned} e_{\pm\varphi} &= p_{-1}^{\pm\varphi}(\pm\varphi/\omega - 2\pi/\omega)^2 + p_{+1}^{\pm\varphi}(\pm\varphi/\omega + 2\pi/\omega)^2 \\ &\quad + (1 - p_{-1}^{\pm\varphi} - p_{+1}^{\pm\varphi})(\pm\varphi/\omega)^2 - b_{\pm\varphi}^2, \\ e_{\pm\varphi} &= \frac{4\pi^2}{\omega^2} (1 - p_0^{\pm\varphi} - \Delta p_{\varphi}^2), \end{aligned}$$

where $\Delta p_{\varphi} = p_{+1}^{\pm\varphi} - p_{-1}^{\pm\varphi} = p_{-1}^{\mp\varphi} - p_{+1}^{\mp\varphi}$. Since from the symmetry $p_0^{+\varphi} = p_0^{-\varphi}$, we can denote MSE for the positively and negatively shifted estimators as

$$e_{\varphi} = \frac{4\pi^2}{\omega^2} (1 - p_0^{\varphi} - \Delta p_{\varphi}^2).$$

Figure 3 (left) shows the actual root-mean-square error (RMSE) and Fig. 3 (right), the predicted RMSE. The three-point model seems to be adequate in this case as well.

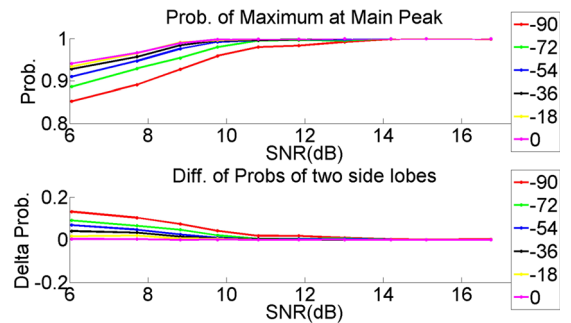


FIG. 1. (Color online) Probability of left and right outlier: the probability that the maximum of the cross-correlation function was detected at the main peak (top) and the differences of the probabilities of outliers induced by two closest side lobes (bottom). Different lines correspond to different phase shift values.

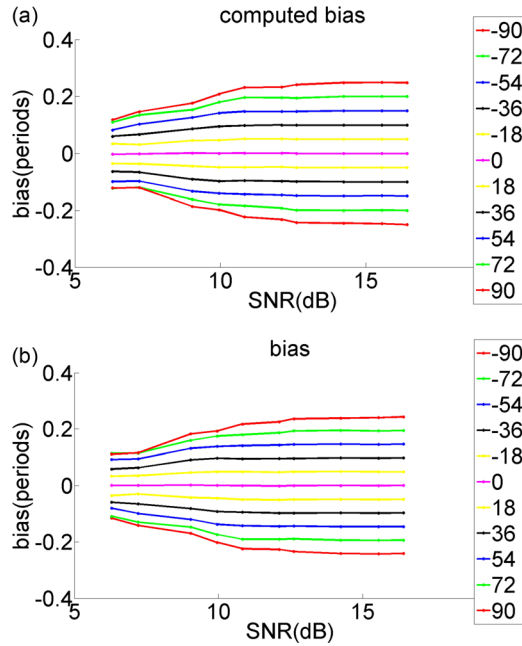


FIG. 2. (Color online) Predicted vs actual bias: The predicted bias computed using estimated outlier probabilities (left) closely follows the actual bias estimated using simulations (right). Different lines correspond to different phase shift values.

Denoting the correlation coefficient for the phase-shifted estimator pair by γ_φ , we can represent the MSE of the unbiased estimator obtained by averaging two biased estimator as

$$e_{\varphi,\gamma} = e_\varphi \frac{1 + \gamma_\varphi}{2}.$$

Therefore, to obtain an improvement in the accuracy, the following inequality should hold:

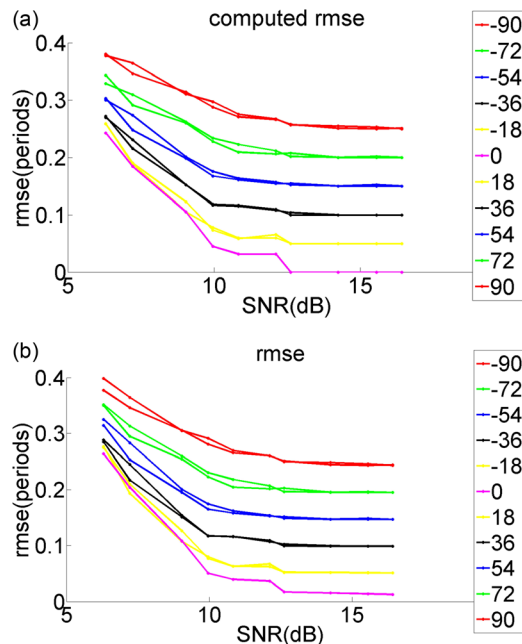


FIG. 3. (Color online) Predicted vs actual RMSE: the predicted RMSE (left) approximately match the RMSE computed using simulations (right). Different lines correspond to different phase shift values.

$$(1 - p_0^\varphi - \Delta p_\varphi^2) \frac{1 + \gamma_\varphi}{2} < (1 - p_0).$$

Ignoring the small second-order term we can simplify to

$$(1 - p_0^\varphi) \frac{1 + \gamma_\varphi}{2} < (1 - p_0).$$

The probability of outliers for the biased estimator could be expressed using the outlier probability of MLE

$$p_{\pm 1}^{\pm\varphi} = p_s \pm \delta_{\pm 1}^\varphi.$$

Although generally $\delta_{+1}^\varphi \neq \delta_{-1}^\varphi$ it is reasonable to assume that, they are very close. Therefore, we can assume that $p_0^\phi \approx p_0$ since

$$\begin{aligned} p_0^\phi &= 1 - p_{+1}^{\pm\varphi} - p_{-1}^{\pm\varphi} = 1 - p_s - \delta_{-1}^\varphi - p_s + \delta_{+1}^\varphi \\ &\approx 1 - 2p_s = p_0. \end{aligned}$$

It follows that an improvement in the accuracy is achieved by reducing the correlation coefficient below the unity. Let us consider the correlation between two events, which jointly cause the largest outlier of size $2\pi/w$. This outlier event happens when noise at both estimators cause the maximum to be detected on a side lobe at the same side of the main peak of the cross-correlation function. Instead of showing a certain degree of independence between actual estimators, we will consider two random variables defined as the difference between noise samples at the peak and a side lobe of each biased estimator. We will show that these random variables are not completely correlated. Therefore, we presume that corresponding biased estimators also have some degree of independence and, thus, they have correlation coefficient less than unity.

For a narrowband signal, the resulting cross-correlation function could be represented as $R_{\pm\varphi}(t) = V(t)\cos(\omega t \pm \varphi)$, where $V(t)$ is the envelope of signal autocorrelation function and ω is the angular central frequency. The filtered noise, samples $N_{\pm\varphi}(t)$ are normally distributed $N_{\pm\varphi} \sim N(0, R(o)\sigma_\eta^2)$ with an autocorrelation function $R(t) = V(t)\cos t(\omega t)$. The probability of an outlier depends on the difference between the heights of the side lobe and the main peak, and the threshold effect appears when that difference is less than the difference between corresponding noise samples. Therefore, we need to characterize the distribution of the random variable corresponding to the difference between filtered noise samples at the nearby extreme points. Let us observe that the correlation between noise samples at the main peak and at either of the side lobes depends only on the relative distance between the side lobes and is equal to $R(2\pi/\omega) = V(2\pi/\omega)$. Therefore, the difference of these noise samples is normally distributed:

$$Z_s = N(t_0) - N(t_s) \sim N(0, 2\sigma_\eta^2(V(0) - V(2\pi/w))),$$

where t_0, t_s are the positions of the main peak and either ($s = \pm 1$) of the closest side lobes in an autocorrelation function. For the phase shift $\pm\varphi$, the position of the main peak is

$t_0^{\pm\varphi} = \pm\varphi/\omega$. Side lobes are located at $t_{+1}^{\pm\varphi} = \pm\varphi/\omega + 2\pi/\omega$ and $t_{-1}^{\pm\varphi} = \pm\varphi/\omega - 2\pi/\omega$. Random variables corresponding to the difference between noise samples at peaks of phase-shifted cross-correlation are

$$Z_{\pm 1}^{\pm\varphi} = N_{\pm 1}^{\pm\varphi} - N_0^{\pm\varphi}.$$

These variables have zero mean and their variance is equal to that of Z_s since the distance between peaks is the same: $2\pi/w$. Since the envelope of cross correlation between $s_{+\varphi}$ and $s_{-\varphi}$ is equal to the envelope of the autocorrelation $V(t)$, we can estimate the covariance among $Z_1^{+\varphi}$ and $Z_1^{-\varphi}$ as

$$\text{Cov}(Z_1^{+\varphi}, Z_1^{-\varphi}) = 2\sigma_\eta^2 \left(V\left(\frac{2\varphi}{w}\right) - V\left(\frac{2\varphi + 2\pi}{w}\right) \right).$$

Therefore, the correlation coefficient is

$$\tilde{\gamma}_\varphi = \frac{V\left(\frac{2\varphi}{w}\right) - V\left(\frac{2\varphi + 2\pi}{w}\right)}{V(0) - V(2\pi/w)} = \frac{h_{2\varphi}}{h_0},$$

where $h_\theta = V(\theta/w) - V(\theta/w + 2\pi/w)$ is the difference between the main peak and the lower side lobe of cross-correlation with the signal phase-shifted by θ . At Fig. 4 this correlation coefficient is compared with the correlation between the actual estimator pairs. It can be seen that for a range of SNR values, both correlations are approximately equal.

If at least a part of the envelope around extreme points is concave, then the correlation coefficient is less than unity. For instance, if the envelope of autocorrelation functions could be approximated by a Gaussian with bandwidth B , that is $V(t) = e^{-t^2/B^2}$, then we would have to keep the phase shifted side lobes away from the envelope's inflection point $B/\sqrt{2}$. Therefore,

$$\frac{2\varphi + 2\pi}{w} < \frac{B}{\sqrt{2}} \rightarrow \varphi < \frac{wB}{2\sqrt{2}} - \pi = \pi \left(\frac{BF}{\sqrt{2}} - 1 \right).$$

If the envelope of the source signal is known, we can use the expression above to find the optimal value of the phase shift to minimize the correlation coefficient. Unfortunately, things are little bit more complicated as we are interested in the tail probabilities of these random variables and as we change phase, the limits on the tail probabilities change.

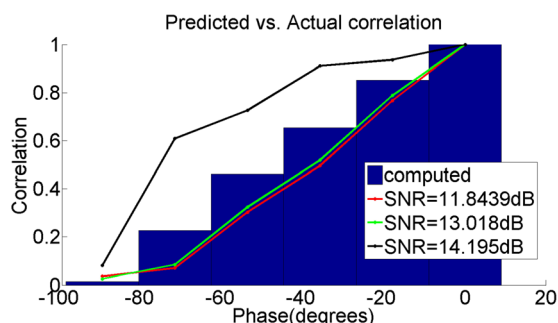


FIG. 4. (Color online) Predicted vs actual correlation coefficient. For SNR = 13 dB, the actual correlation coefficient closely follows predicted values.

III. FUSION OF BIASED ESTIMATORS USING REGRESSION

Using a set of different phase shift values, we can construct a feature space that will supply even more information regarding the position of the ping within the received signal. Then, using this feature space, we can train a regression model to predict an offset between the value of the MLE and the true location of the source signal in a received echo.

First, we construct a family of filters by employing several phase-shifted unmatched filter pairs

$$\{\varphi_i\}_{i=-n}^n, \text{ where } \varphi_i = -\varphi_{-i}.$$

Combined with the matched filter, this gives a family of $2n + 1$ filters that can be applied to the received signal to obtain $2n + 1$ estimates defined as

$$\hat{t}_i(x, s) = \hat{t}_{\varphi_i}(x, s) = \arg \max_t C_{\varphi_i}(t), \quad i = -n, \dots, n.$$

These $2n + 1$ values constitute a feature space that contains enough information to improve accuracy of ToA estimation for a wide range of SNR values. We explore two regression methods for extracting this information to obtain robust semi-coherent ToA estimator. The employed regression methods are neural network and support vector regression.¹⁸ Both regression methods use Gaussian as a radial base function (RBF) kernel¹⁹ with exact parameters tuned by cross-validation process. A resulting regression model is used for correcting a possible error in the MLE due to misidentification of the main peak in the cross-correlation function. This error is corrected by an additive offset Δt_0 which is predicted based on the output of biased estimators \hat{t}_i . Since we are interested only in predicting the relative offset, feature vectors for training, validation, and test sets are normalized by subtracting the MLE from the rest of biased estimators. Therefore, the input vector of features supplied to a regression becomes

$$\hat{t}_i^n = \hat{t}_i - \hat{t}_0.$$

The simulation process proceeds as follows. About 20 000 of random samples are generated using ten SNR values within the semi-coherent SNR range. A bank of 21 filters corresponding to ten pairs of phase shift filters and the zero-shifted (matched) filters is used to produce a feature vector of 21 values. Then these vectors are normalized by subtracting the value of MLE as described above. The resulting data set is split into training, validation and test sets. The true value of the corrective offset is computed as a difference between the MLE value and known true value of the lag. The samples corresponding to all SNR values are mixed together for training and validation set while test set samples are kept grouped by the SNR value. The training set is used for training two regression models and the validation set is employed for tuning the regression parameters (the spread parameter for RBF NN regression, and the threshold parameter for SVR).

The resulting regression models are used to evaluate the test error for each simulated SNR values separately. The

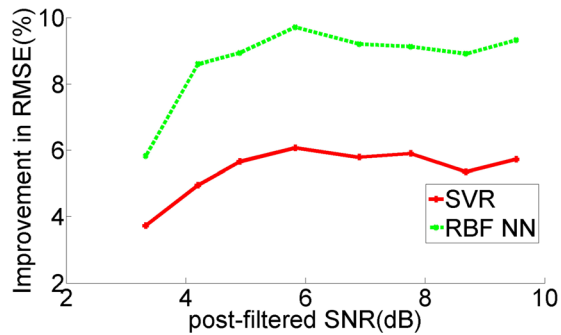


FIG. 5. (Color online) Relative improvement in RMSE compared to the conventional MLE ToA estimator. Both regression methods provide significant improvement for a range of semi-coherent SNR values. However, the RBF Neural Network Regression gives better results (up to 10% improvement) for all tested SNR values. No explicit knowledge on operational SNR value is required as regression models are trained using a mix of near-threshold SNR values.

resulting relative improvement in RMSE compared to the standard MLE ToA estimator is shown in Fig. 5. The neural networks-based regression method is found to be the best performing methods resulting in up to 10% improvement in RMSE for a range of near-the-threshold SNR values.

IV. SUMMARY AND CONCLUSIONS

We have presented a biosonar-inspired method for the problem of the semi-coherent ToA estimation. The method is based on a regression modeling for fusion of a multitude of biased but only partially correlated estimators. These estimators are obtained using a filter bank of phase shifted unmatched filters that are easily constructed from the source waveform. The bias, MSE, and pairwise correlation between these biased estimators were analyzed using simple three-point model. The simulation results were used to compare predicted and actual values of these statistics. Between two tested regression methods, the neural network regression using Gaussian RBFs was found to be superior, resulting in up to 10% improvement in RMSE compared to the conventional matched filter based estimator. The described method does not rely on explicit knowledge of operational SNR values and, thus, could be employed as a robust ToA estimator in the presence of the threshold effect. The proposed approach could be extended further by considering usage of more advanced machine learning techniques for fusion of partially correlated estimators. For instance, it might include an explicit classification of outlier events according to the originating peaks of cross-correlation function. A similar approach could be applied to the problem of semi-coherent signal detection by employing the described feature space for detecting the presence of signal in a heavy noise. The practical implication of our work includes an increase in the

operational range and/or a reduction in required operational power for remote sensing devices operating under high noise (e.g., underwater sonar or underground exploration by low power signals).

ACKNOWLEDGMENT

This work was supported in part by the U.S. Army Research Office under Grant No. W911NF-07-1-0256.

- ¹M. I. Skolnik, *Introduction to Radar Systems* (McGraw-Hill, New York, 1962).
- ²S. M. Kay, *Fundamental of Statistical Signal Processing* (Prentice Hall, Englewood Cliffs, NJ, 1993).
- ³Harry L. Van Trees, *Detection, Estimation and Modulation Theory* (Wiley, New York, 2004).
- ⁴R. N. McDonough and A. D. Whalen, *Detection of Signals in Noise* (Academic, San Diego, 1995).
- ⁵B. M. Sadler and R. J. Kozick, "A survey of time delay estimation performance bounds," *Fourth IEEE Workshop on Sensor Array and Multichannel Processing* (2006), pp. 282–288.
- ⁶A. Zeira and P.M. Schultheiss, "Realizable lower bounds for time delay estimation—Part II: Threshold phenomena," *IEEE Trans. Signal Process.* **4**(5), 1001–1007 (1994).
- ⁷E. W. Barankin, "Locally best unbiased estimates," *Ann. Math. Stat.* **20**, 477–501 (1949).
- ⁸A. Pinkus and J. Tabrikian, "Barankin bound for range and Doppler estimation using orthogonal signal transmission," in *Proceedings of IEEE Radar Conference* (2006), pp. 94–99.
- ⁹P. Woodward, *Probability and Information Theory, with Applications to Radar* (McGraw-Hill, New York, 1953).
- ¹⁰A. Apartsin, L. N. Cooper, and N. Intrator, "SNR-dependent filtering for time of arrival estimation in high noise," *Proceedings of IEEE Machine Learning for Signal Processing (MLSP)* (2010), pp. 427–431.
- ¹¹A. Apartsin, L. N. Cooper, and N. Intrator, "Biosonar-inspired source localization in low SNR," *Proceedings of BIOSIGNALS' 2011*, pp. 399–404.
- ¹²L. R. Varshney and D. Thomas, "Side lobe reduction for matched filter range processing," *Proceedings of IEEE Radar Conference* (2003), pp. 446–451.
- ¹³L. Yu, N. Neretti, and N. Intrator, "Multiple ping sonar accuracy improvement using robust motion estimation and ping fusion," *J. Acoust. Soc. Am.* **119**(4), 2106–2113 (2006).
- ¹⁴J. A. Simmons and R. A. Stein, "Acoustic imaging in bat sonar: Echolocation signals and the evolution of echolocation," *J. Comp. Physiol.* **135**(1), 61–68 (1980).
- ¹⁵T. Kimchi, M. Reshef, and J. Terkel, "Evidence for the use of reflected self-generated seismic waves for spatial orientation in a blind subterranean mammal," *J. Exp. Biol.* **208**(5), 647–659 (2005).
- ¹⁶N. Neretti, M. I. Sanderson, J. A. Simmons, and N. Intrator, "Time-frequency computational model for echo-delay resolution in sonar images of the big brown bat, *Eptesicus fuscus*," *J. Acoust. Soc. Am.* **113**(4), 2137–2145 (2003).
- ¹⁷D. R. Pauluzzi and N. C. Beaulieu, "A comparison of SNR estimation techniques for the AWGN channel," *IEEE Trans. Commun.* **48**(10), 1681–1691 (2000).
- ¹⁸P. D. Wasserman, *Advanced Methods in Neural Computing* (Van Nostrand Reinhold, New York, 1993), pp. 155–161.
- ¹⁹S. S. Keerthi and C. J. Lin, "Asymptotic behaviors of support vector machines with Gaussian kernel," *Neural Comp.* **15**(7), 1667–1689 (2003).
- ²⁰N. Neretti, N. Intrator, and L. N. Cooper, "Adaptive pulse optimization for improved sonar range accuracy," *IEEE Signal Process. Lett.* **11**(4), 409–412 (2004).